Vol. 13(9), pp. 365-380, September 2019
DOI: 10.5897/AJEST2019.2717
Article Number: A4CCBE561869
ISSN: 1996-0786
Copyright ©2019
Author(s) retain the copyright of this article
http://www.academicjournals.org/AJEST

ACADEMIC JOURNALS
expand your knowledge

African Journal of Environmental Science and Technology

Full Length Research Paper

Non-linear equilibrium and kinetic study of the adsorption of 2,4-dinitrophenol from aqueous solution using activated carbon derived from olives stones and cotton cake

Aurelien Bopda[1], Donald Raoul Tchuifon Tchuifon[1], Nche George Ndifor-Angwafor[1], Giscard Doungmo[2] and Anagho Solomon Gabche[1,3*]

[1]Research Unit of Noxious Chemistry and Environmental Engineering, Department of Chemistry, Faculty of Science, University of Dschang, P. O. Box 67, Dschang, Cameroon.
[2]Institute on Inorganic Chemistry, Christian-Albrebrechts-Universität zu Kiel, Max-Eyth-Straβe 2, 24118 Kiel, Germany.
[3]Department of Chemistry, Faculty of Science, University of Bamenda, P. B. Box 39 Bambili, Cameroon.

Received 2 June, 2019; Accepted 14 August, 2019

Olives stones and cotton cakes have been investigated as a cheap and available precursor used for the production of novel carbon using potassium hydroxide as chemical activating agent with 2:1 impregnation ratio at 1.5 M KOH. Carbonization was performed at 450°C for one hour. The activated carbons NOK and MK3 were characterized by Iodine Number, Fourier Transform Infrared (FTIR) spectroscopy, EDX Analysis, Scanning Electron Microscopy (SEM), X-ray Diffraction (XRD) Analysis and Proximate Analysis (pH_{ZCN}, pH, volatile matter, fixed carbon). The effects of initial sorbate concentration and contact time on adsorption were evaluated. Errors analysis methods were used to evaluate the experimental data: Correlation coefficient (R^2), chi-square (χ^2), average relative error (ARE), sum of absolute errors (EABS) and root mean square error (RMSE) values were tested to find the best fitting isotherm. Elovich models provide the best fit in the uptake of 2,4-dinitrophenol by activated carbons NOK and MK3. Thus, among the isotherm models studied, it appears that the Dubinin-Radushkevich and Temkin (two parameters), Sips (three parameters) and Baudu (four parameters) models describe better the adsorption data. Error analysis showed that the models with two parameters better described the adsorption of 2,4-diniphenol data compared with the three parameter and four-parameter models.

Key words: 2,4-dinitrophenol, activated carbon, cotton cake, olives stones, isotherms, kinetics.

INTRODUCTION

In the present century, environmental problems have increased because of increasing population, consumption of natural habitat, and development of industrialization. These are causes for rapidly destroying the ecological

*Corresponding author. E-mail: sg_anagho@yahoo.com.

Author(s) agree that this article remain permanently open access under the terms of the Creative Commons Attribution License 4.0 International License

system and clean resources rapidly. Environmental pollutants may have organic and inorganic origins. Phenolic compounds as a class of organics which are generated by petroleum and petrochemical, coal conversion, phenol producing industries, and other chemical processes, are common contaminants in wastewater. 2,4-dinitrophenolas one of the vital nitro aromatic compounds is among the most toxic substances, and are commonly used in the manufacture of wood preservatives, explosives, pesticides, dyes, wood preservation agents, plasticizers, and pharmaceuticals (Tchieda et al., 2010). The maximum permissible concentration of nitrophenol in wastewater of 1 µg/L which was set by United State Environmental Protection Agency (USEPA) (Berardinelli et al., 2008; Mubarik et al., 2012). It has arisen as a serious problem in terms of its carcinogenicity and high toxicity as well as creating unpleasant taste and odor in water resources. 2,4-diniphenol has excessive impact on human health and causes nausea, sweating, vomiting, headaches, dizziness and weight loss. Additionally, skin lesions and cataracts are formed by exposure to 2,4-dinitrophenol (Miranda et al., 2006). 2,4-dinitrophenol toxin also affects the bone marrow, cardiovascular system and Central Nervous system (Luan and Plaisier, 2004). Therefore, the treatment of effluent containing such nitrophenols is of interest due to its harmful impacts in receiving waters. Various methods have been applied in the removal of nitrophenols from water and wastewater. These methods include distillation, coagulation, electrocoagulation (Bazrafshan et al., 2012), biological treatment, catalytic oxidation, ozonation (Biglari et al., 2017), solvent extraction, and adsorption (Tchieda et al., 2010; Mubarik et al., 2012; Tchuifon et al., 2014; Muhammad, 2018; Bopda et al., 2018).

Out of these methods, adsorption appears to be most widely used for 2,4-dinitrophenol removal (Muhammad, 2018; Bopda et al., 2018). Activated carbon adsorption has been cited by the USEPA as one of the best available environmental control technologies (Hamdaoui et al., 2005) because it is a cleaner, more efficient and cheap technology.

Previously, research working on various precursors for activated carbon has studied the possibility and efficiency of utilization of agricultural fibres as an adsorbent for Phenolic compounds removal in polluted water. Some of the low cost agricultural wastes that have been studied include: rice husk (Tchuifon et al., 2014; Okieimen et al., 2007; Ndifor-Angwafor et al., 2017), palm kernel shell (Abechi et al., 2013), lapsi (*Choerospondias axillaris*) seed stone (Sahira and Bhadra, 2013), cola nut (*cola acuminata*) shells (Ndi et al., 2014), bitter kola (*Garcinia kola*) nut shells (Kuete et al., 2018) and mixture of *Ayous* sawdust and C*ucurbitaceae* peelings (Ngakou et al., 2018). These agricultural wastes which are used to produce the activated carbons are generated in large quantities and in some cases might become difficult to dispose and have proven very effective in the adsorption of phenolic compounds removal in water.

The performance of an adsorbent can be studied from adsorption kinetics and isotherm data. The equilibrium correlation is developed using equilibrium isotherms. Also isotherms express sorbent interactions with the surface of adsorbent, that is, whether it is monolayer or multilayer sorption (Foo and Hameed, 2010). An analysis of the kinetic data is important because the kinetics describe the uptake rate of adsorbate, which in turn controls the resident time in the adsorbent-solution interface (Junxiong and Lan, 2009).

The aim of the present research was to explore the performance of activated carbon derived from a mixture of cotton cakes and olive stones for the adsorption of 2,4-dinitrophenol under different operating conditions including pH, contact time and initial concentration. The application of non-linear forms of equilibrium isotherms was to determine the appropriate isotherm for the purpose and kinetic studies were performed to check reaction nature of the adsorption phenomenon. Error analysis based on five different error functions was also performed.

MATERIALS AND METHODS

Cotton cake and olive stone were collected respectively from Zamay (Nord region Cameroon) and Bangangte (west region Cameroon) (Figure 1) and processed (Sugumaran et al., 2012). They were cut into small pieces of about 0.5 to 1 cm in size, dried under sunlight until all the moisture was evaporated.

Preparation of activated carbon

Preparation of activated carbon from olive stones (NOK) and mixture of cotton cake and olive stones (MK3) were carried out by chemical activation process with KOH activating agent at concentration 1.5 M. 120 g of different material were inserted into each of five flasks, and activating agent solutions with impregnation ratios was 2/1 (w/w) were added. The mixture was allowed for 30 min activation to take place before being dried in an oven set 105°C for 48 h. The impregnated samples were carbonized for 1 h at 450°C, at a heating rate of 5°C min^{-1}. After impregnation and carbonization, the pyrolysed carbons based KOH were leached with 1% HCl (v/v) for 2-3 H, were washed several times with distilled water until a neutral pH for the two carbons based KOH was achieved. Later, the carbon paste was dried in an oven at 110°C for at least 24 h which were later converted to powdered activated carbon of particle size lower than 100 µm and pestle before application. The prepared activated carbon was characterized by the adsorption capacity towards iodine using the standard test method for the determination of iodine number of activated carbon (ASTM, 2006).

Characterization of activated carbons

The activated carbons were characterized by Fourier transform-infrared (FTIR) spectroscopy, scanning electron microscopy (SEM), X ray diffraction (XRD), EDX analysis and proximate analysis (pH_{PZC}, pH, Bulk density, moisture content, ash content, volatile

Figure 1. Photography of selected lignocellulosic wastes (A: cotton cake; B: olive stone).

matter, fixed carbon content and matter soluble in water) by the method used by Abechi et al. (2013); Pongener et al. (2015); Abechi et al. (2013) and Pongener et al. (2015).

Batch equilibrium experiments and analytical method

Stock solution of 2,4-dinitrophenol at the concentration of 500 mg L^{-1} was prepared by dissolving 0.125 g of 2,4-dinitrophenol in 0.250 L of distilled water. Experimental solutions at desired concentrations were obtained by dilution of the stock solution with distilled water pre-adjusted to pH range from 2.0 - 7.0 with a 0.01 M HCl or NaOH solution. The different contact times varied between 0 and 180 min. The initial concentrations of the experimental solutions of 2,4-dinitrophenol were 20, 25, 30, 35, 40, 45 and 50 mg L^{-1}. 30 ml of the experimental solutions were placed in bottles and then 0.05 g prepared activated carbon was added to each bottle. After agitation for about during equilibrium time, the solution was filtered, and the filtrate analyzed to obtain the residual concentration 2,4-dinitrophenol by using the UV/Vis spectrophotometer at λ_{max} value of 320 nm.

Modelling theoretical background

Tables 1 and 2 summarizes the non-linear forms of the two, three and four parameter isotherms models and non-linear forms of kinetics models used respectively in this study.

Error functions analysis

In general, plus values of errors function are low it means more there is an agreement between the experimental and calculate data and more the model converges and becomes favourable, their functions are listed in Table 3.

RESULTS AND DISCUSSION

Characterization of activated carbons

Burn-off, yield and iodine number

Table 4 contains the burn-off, yield and iodine number for various activated carbons. It is deduced from this table that the yield obtained by the activation process of activated carbons of olives stone and mixed precursors has burn-off from 32 to 50% which, indicates that these carbons have microporous structure (Bansal et al., 1988).

Iodine number is defined as the number of milligrams of iodine absorbed by one gram of activated carbon powder. Table 2 gives the values of the iodine number of the samples. The iodine numbers of activated carbons prepared in this investigation lie between 520.00-591.00 mg g^{-1}. The higher Iodine number of the activated carbon is attributed to the presence of large microporous structure that results due to the reactivity of the activating agent KOH. Generally, the higher the iodine number, the greater the sorption capacity. The iodine number recommended as a minimum by the American Water Works Association for a carbon to be used in removing low molecular weight compounds is 500 (ASTM, 2006). The two factors that determine good iodine number are activation temperature and raw materials. This suggests that surface area increases in terms of microscopic pores. Iodine adsorption is usually associated with micro pores because of the small size of iodine molecule.

The proximate analysis

The proximate analysis was performed according to the ASTM methods was examined and shown in Table 5.

SEM analysis

The surface morphology of the activated carbons was studied by SEM techniques. In the chemical activation process, new pores are formed due to the reaction between carbon and the activating agents (Arvind and Hara, 2015). SEM micrographs of NOK and MK3 are shown in Figure 2. Figure 2 shows that the adsorbent

Table 1. Non-linear forms of the two, three and four parameter isotherms.

Parameter	Isotherms	Nonlinear forms	References
Two	Langmuir	$Q_e = \frac{Q_m K C_e}{1 + K C_e}$	Al-Duri and McKay (1988)
	Freundlich	$Q_e = K_f C e^{1/n}$	
	Dubinin-Radushkevich	$Q_e = Q_m \exp(-K\varepsilon^2)$; $\varepsilon = RT \ln(1+1/C_e)$;	Gunay et al. (2007)
	Temkin	$Q_e = Q_m \frac{RT}{\Delta Q} \ln(AC_e)$	Ringot et al. (2007)
	Jovanovic	$q_e = q_m(1 - e^{k_j C_e})$	Rania and Yousef (2015)
Three	Redlich-Peterson	$q_e = \frac{AC_e}{1 + BC_e^{\beta}}$	
	Sips	$q_e = \frac{K_s C_e^{\beta}}{1 + a_s C_e^{\beta s}}$	
	Toth	$\frac{q_e}{q_m} = \frac{K_e C_e}{[1 + (K_L C_e)^n]^{1/n}}$	Ayawei et al. (2017)
	Hill	$q_e = \frac{q_{SH} C_e^{nH}}{K_D + C_e^{nH}}$	
	Kahn	$Q_e = \frac{Q_{max} b_k C_e}{(1 + b_k C_e) a_k}$	
Four	Fritz-Schlunder	$q_e = \frac{q_{mFSS} K_{FS} C_e}{1 + q_m C_e^{MFS}}$	Yaneva et al. (2013
	Baudu	$q_e = \frac{q_m bo C_e^{1+x+y}}{1 + bo C_e^{1+x}}$	McKay et al. (2014)
	Marczewski-Jaroniec	$q_e = q_{MMJ}(\frac{(K_{MJ} C_e)^{n_{MJ}}}{1 + (K_{MJ} C_e)^{n_{MJ}}})^{M_{Mj}/n_{MJ}}$	Ayawei et al. (2017)

Table 2. Non-linear forms of kinetics models.

Kinetics	Non-linear form	References
Pseudo-first-order	$q_t = q_e(1 - e^{-k_1 t})$	Ho (2004)
Pseudo-second-order	$q_t = \frac{k_2 q_e^2 t}{1 + k_2 q_e t}$	Ho and Mckay (1998)
Elovich	$q_t = \frac{ln(\alpha\beta)}{\beta} + \frac{ln\, t}{\beta}$	Chien and Clayton (1980)
Intraparticle diffusion	$Q_t = K_{id} t^{1/2} + C$	Weber and Morris (1963)

have rough texture with heterogeneous surface and a variety of randomly distributed pore size. The SEM images of NOK and MK3 are porous in appearance. Sample MK3 presents pores which are, apparently, more open (broad) compared to NOK material, which is explained by a mixture precursors used in this material. Sample MK3, the mixture of cottons cake and olives stone activated reduces the orderly pores development on the surface of the activated carbons. This can be a result of impurities such as tar produced by precursor in the mixture that could clog the pores and inhibit good pore structure development since the amount of activating agent stays constant during the production process.

EDX analysis

For the activated carbon having heterogeneous surfaces, EDX analysis was carried out on several zones of the

Table 3. Error functions and their equations.

Error function	Abbreviation	formula	References
Residual root mean square error	RMSE	$\sqrt{(\frac{1}{n-2}\sum_{i=1}^{n} q_{e,exp} - q_{e,calc}))^2}$	Sugumaran et al. (2012)
Hybrid fractional error function	HYBRID	$\frac{100}{n-p}\sum_{i=1}^{n}\frac{(q_{e,i,means} - q_{e,i,calc})^2}{q_{e,i,meas}}$	Mckay et al. (2014)
Average relative error	ARE	$\frac{100}{n-p}\sum_{i=1}^{n}\frac{(q_{e,i,calc} - q_{e,i,means})}{q_{e,i,meas}}$	
Nonlinear chi-square test	χ^2	$\sum_{i=1}^{n}\frac{(q_{ecal} - q_{emeas})^2}{q_{emeas}}$	(Chan et al., 2012)
Sum of absolute errors	EABS	$\sum_{i=1}^{p}(q_{e,i,means} - q_{e,i,calc})$	Ayawei et al. (2017)
Coefficient of determination	R^2	$\frac{\sum_{i=1}^{n}(q_{ecal} - q_{mexp})^2}{\sum_{i=1}^{n}(q_{ecal} - q_{mexp})^2 + (q_{ecal} - q_{mexp})^2}$	

Table 4. Burn-off, yield and iodine number for various activated carbons.

Variable	Yield (%)	Burn-off (%)	Iodine number (mg g^{-1})
NOK	62.88	37.12	523.46
MK	62.22	37.78	590.49

Table 5. The proximate analysis composition of NOK and MK3.

Property	NOK	MK3
pH_{ZCN}	5.67	6.01
pH	6.88	6.98
Bulk density (kg m^{-3})	471.60	617.20
Moisture content (%)	3.00	2.00
Ash content (%)	16.80	4.00
Volatile mater (%)	28.68	32.00
Fixe carbon content (%)	51.52	62.00
Matter soluble in water	0.47	0.38
Elements (%)		
C	92.49	94.72
O	7.51	5.28

material. The results of EDX analysis of studied (Figure 3) showed that these materials primarily consist of carbon and oxygen in different proportions. The presence of oxygen may be attributed to the little amount of moisture in the carbon. The carbon content in activated carbons from mixed precursors is greater than that from the simple precursors and oxygen percentage in activated carbons from simple precursors, is greater than in that from the mixed precursors. The high carbon % and low oxygen % in activated carbons are attributed to the volatilization of oxygen and hydrogen atoms. The results of typical EDX elemental microanalysis of the activated

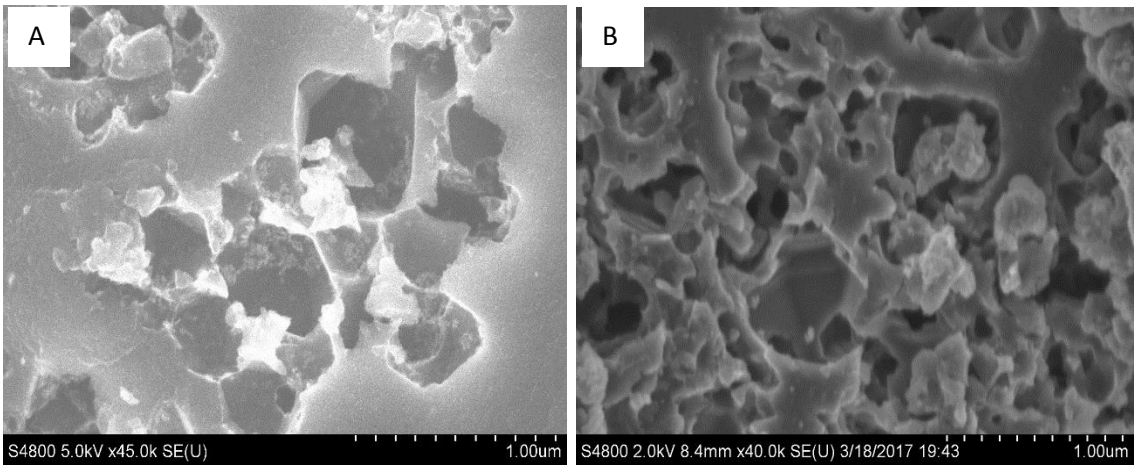

Figure 2. SEM micrographs of activated carbon of samples: A) NOK; B) MK3.

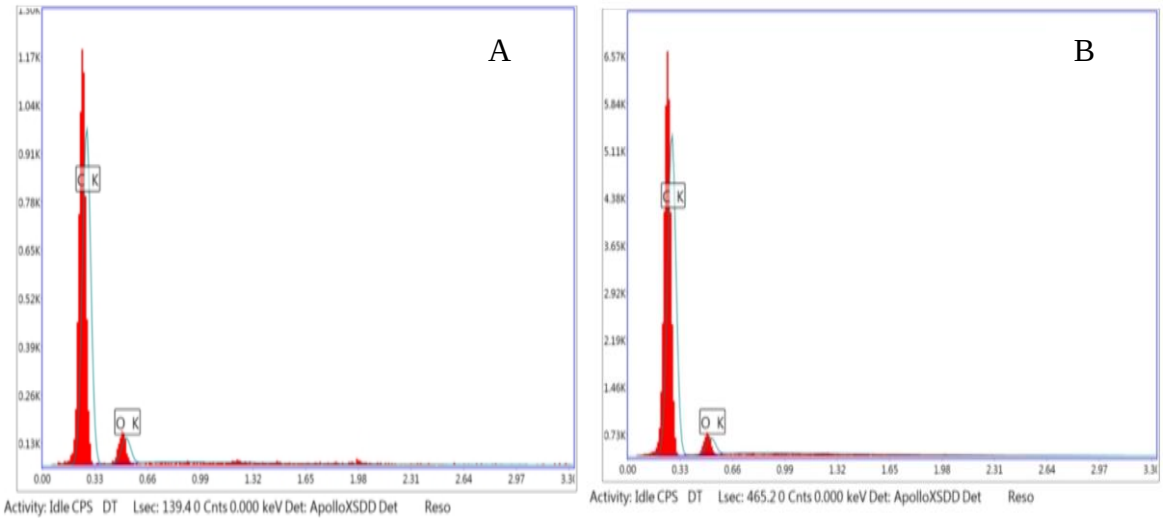

Figure 3. EDX elemental microanalysis of activated carbon of samples (A: NOK, B: MK3).

carbons in Figure 3 and the percentage of the element present in the different activated carbons is given in Table 5.

Fourier transform Infra-red spectroscopy (FTIR)

The FT-IR spectroscopy was used to determine the various functional groups present in adsorbent materials. The result depicts the absorbance spectra of the NOK and MK3 shown in Figure 4. The main components of the raw material olive stones are hemicellulose, cellulose, and lignin which have an aromatic character. The wide absorption at 3300 cm^{-1} is assigned to the O-H stretching vibration mode in alcohol and phenol. The vibration band at 3319 cm^{-1} was attributed to the acetylenic stretching. The region between 2915 and 2849 cm^{-1} have two intense peaks assigned to C-H stretching vibrations. The adsorption band at 1580 cm^{-1} is attributed to quinonic, monosubstituted alkene and carboxylate structures mean while the adsorption band at 1735 cm^{-1} is attributed to a carboxylic tautomeric structure (C=O). The bands located at 1100 and 1120 $cm^{-1}$are attributed to C-O stretching vibrations in alcohols and phenols (Virote et al., 2005). The bands observed between 800 and 500 $cm^{-1}$are due to out of plane deformation mode of C-H for alkenes aromatic rings. Bands observed at 600 and 400 $cm^{-1}$are ascribed to C-H in out-of-plane bending in the edges of aromatic rings or are assigned to cyclic amides (El-Hendawy, 2006). This behavior suggests that the activated carbon is mainly an aromatic polymer of activated carbon. The most important bands and peaks

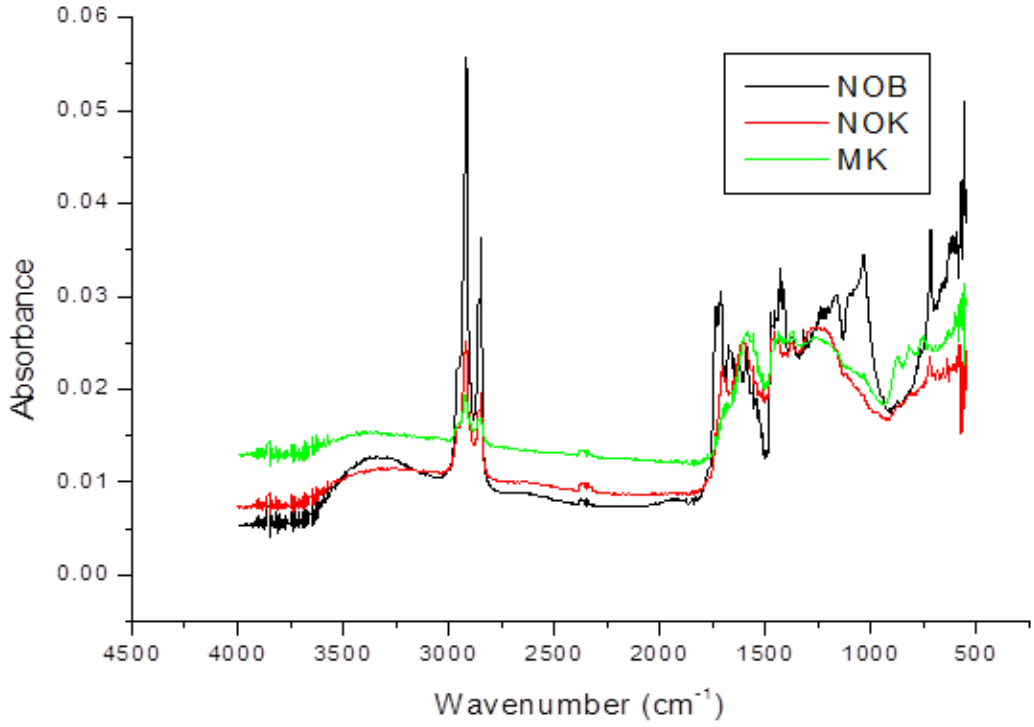

Figure 4. Fourier transform infrared spectra of olive stones (NOB), olive stones based activated carbon (NOK) and mixed biomass based activated carbon (MK3).

appearing on the spectrum of NOB are the same present on NOK but with low O-H and C-H intensities peak and this can be explained by carbonization which is at the origin of the atoms of C, O, H in the form of CO_2, H_2O, and aldehyde. These results are in agreement with these of Boehm titrations. The loss of the band of adsorption located at located at 1100 and 1120 cm^{-1}characteristic of the C-O can be explained by the fact why the process of chemical activation causes sometimes cuts of the chemical bonds and eliminates several volatiles substrates. The spectra of NOK have the same peaks. The most important bands and peaks appearing on the spectrum of MK3 are the same presented on NOK but with high intensities.

X-ray diffraction (XRD) analysis

The results of powder X-ray diffraction obtained for olive stones (NOB), and the activated carbons (NOK and MK) are presented in Figure 5. The existence of broad peaks indicates that the materials are amorphous (Omri and Benzina, 2012). For the olive stones biomass, a sharp peak appeared at 2θ = 18° and small sharp peak at 2θ = 24°. This signifies an increasing regularity of crystalline structure, which will result in a better layer alignment. The absence of a sharp peak reveals that the activated carbon prepared from NOB and mixed biomass are mainly amorphous (Omri and Benzina, 2012). The disappearance of the sharp peaks is mainly due to the removal of lignin and the breakdown of the ester bonds between lignin and other components during KOH pretreatment and carbonization of the biomass. The amorphous nature of our activated carbon is an advantageous property for well-defined adsorbent. However, the small sharp peaks presented by the X-ray graph of NOK (2θ = 21°) indicates a very low crystallinity on this activated carbon resulting from better layer alignment. The sharp peaks are due to the presence of potassium carbonate and potassium oxide (Lillo-Rodenas et al., 2003). The broad peak found at approximately 19° for the two carbons confirm that the samples are nongraphited, and can have a high microporous structure (Zhao et al., 2009).

Adsorption study

Adsorption kinetics modeling

Study of adsorption kinetics is important because the rate of adsorption (which is one of the criteria for determining efficiency of adsorbents) and also the mechanism of adsorption can be obtained from non-linear kinetic studies. In this study, kinetic data were fitted with four models (pseudo-first-order, pseudo-second-order,

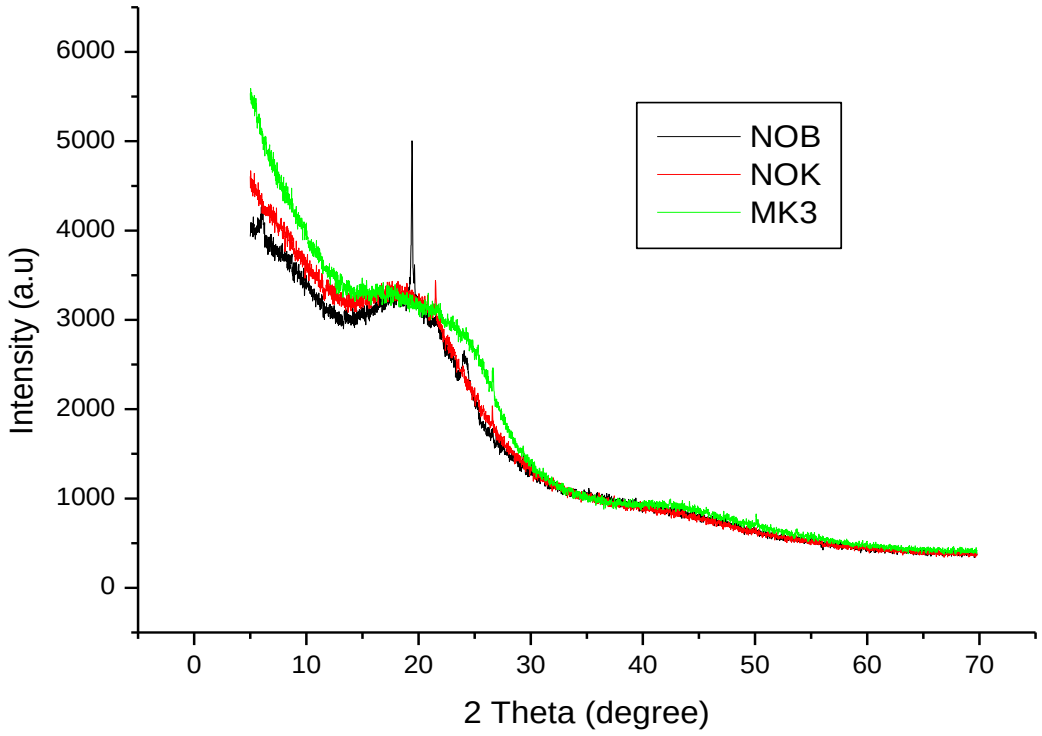

Figure 5. X-ray Diffraction of olive stones (NOB), olive stones based activated carbon (NOK) and mixed biomass based activated carbon (MK3).

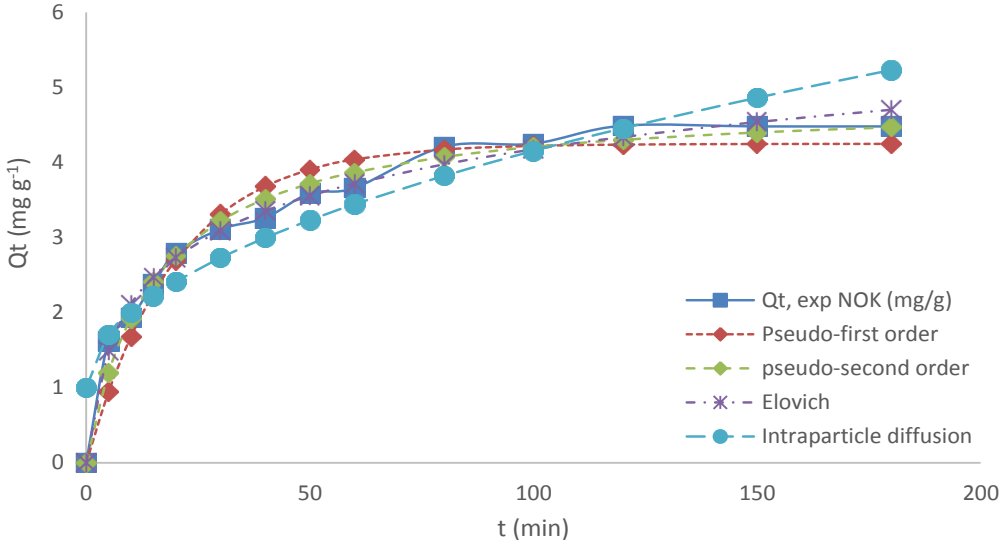

Figure 6. Comparison of measured and calculated Q_e values for kinetics onto activated carbon NOK.

intraparticle diffusion and Elovich model). Figures 6 and 7 shows the variation of the amount of adsorbed (q_t) as a function of time.

Table 6 shows the kinetic parameters obtained using the non-linear method. As can be seen from Table 6, the coefficients of determination for all models are very good. Elovich model equation's χ^2 values were lower than 0.232. Elovich models provide the best fit in the uptake of 2,4-dinitrophenol for any adsorbent, with smaller error values (ARE, EABS, RMSE and HYBRID) onto the

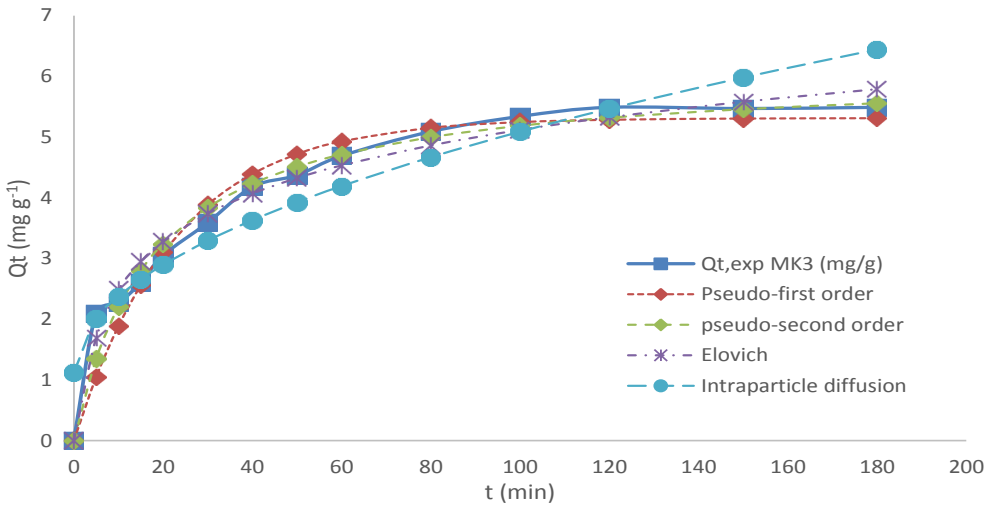

Figure 7. Comparison of measured and calculated Qe values for kinetics onto activated carbon MK3.

Table 6. Optimum kinetics parameters and their statistical comparison values onto activated carbon MK3.

N°	Model	Constant	Value	R^2	RMSE	χ^2	Hybrid	Area	EABS
MK3									
1	Pseudo first order	Q_e (mg g^{-1}) K_1 (1 min^{-1})	5.313 0.044	0.959	1.300	1.239	6.303	8.446	0.062
2	Pseudo second order	Q_e (mg g^{-1}) K_2 (g $min^{-1}mg^{-1}$)	6.104 0.009	0.979	0.895	0.487	3.052	5.670	2.162
3	Elovich	α (mg $g^{-1}min^{-1}$) β (g mg^{-1})	1.002 0.874	0.966	0.823	0.232	2.009	6.054	2.086
4	Intraparticle diffusion	K_p (mg $g^{-1}min^{-0.5}$) C (mg g^{-1})	0.397 1.118	0.889	1.883	1.592	4.307	7.594	5.480
NOK									
1	Pseudo first order	Q_e (mg g^{-1}) K_1 (1 min^{-1})	4.248 0.050	0.954	1.086	0.653	4.523	9.207	3.253
2	Pseudo second order	Q_e (mg g^{-1}) K_2 (g $min^{-1}mg^{-1}$)	4.844 0.014	0.984	0.612	0.199	1.481	4.581	1.645
3	Elovich	α (mg $g^{-1}min^{-1}$) β (g mg^{-1})	0.944 1.116	0.983	0.460	0.067	0.616	3.566	1.407
4	Intraparticle diffusion	K_p (mg $g^{-1}min^{-0.5}$)	0.315	0.879	1.567	1.389	3.488	7.926	4.571

different adsorbents. This suggests that the Elovich sorption mechanism is predominant and that the overall rate, extent of surface coverage and activation energy are favored at lower adsorbents amounts and the adsorption process appears to be controlled by the chemical process (Khalil et al., 2016). However, the Pseudo second order model can also be considered as an alternative option in defining the kinetic processes involved in this adsorption phenomenon. The Elovich equation was used successfully to describe second-order kinetics assuming that the actual solid surfaces are energetically heterogeneous (Demirbas et al., 2008).

Adsorption isotherm modelling

Non-linear regression can be a powerful alternative to linear regression because it offers the most flexible curve fitting functionality. For non-linear isotherm model, sum of square must be minimized by an iterative method. The non-linear regression line is the line that minimizes the sum of squared deviations of prediction (also called the sum of squares error). The smaller the standard error of the estimate the more accurate the prediction. The parameters of the different isotherms obtained by minimizing each error function and maximizing R^2 in an

Table 7. Optimum isotherm parameters and their statistical comparison values for two-parameter models.

N°	Model	Constants	Value	R^2	RMSE	χ^2	Hybrid	ARE	EABS
MK3									
1	Langmuir	Q_{max} (mg g^{-1}) K_L (L mg^{-1})	9.112 0.053	0.977	0.267	0.014	0.288	1.865	0.663
2	Freundlcih	K_F (L mg^{-1}) n	1.299 2.339	0.956	0.363	0.027	0.549	2.510	0.878
3	Temkin	a (L mg^{-1}) b (J mol^{-1})	1.760 1769.4	0.571	0.731	0.111	2.517	4.004	4.306
4	DR	Q_{max} (mgg^{-1}) K (L mg^{-1})	8.079 0.002	0.986	0.209	0.008	0.166	1.428	0.525
5	Jovanovic	Q_{max} (mg g^{-1}) K_J (L mg^{-1})	6.754 -0.060	0.983	0.225	0.010	0.198	1.562	0.567
NOK									
1	Langmuir	Q_{max} (mg g^{-1}) K_L (L mg^{-1})	13.867 0.014	0.919	0.549	0.080	1.680	4.276	1.102
2	Freundlcih	K_F (L mg^{-1}) n	0.339 1.369	0.917	0.555	0.081	1.681	4.568	1.181
3	Temkin	a (L mg^{-1}) b (J mol^{-1})	0.156 929.803	0.994	0.561	0.084	1.811	3.340	1.078
4	DR	Q_{max} (mg g^{-1}) K (L mg^{-1})	7.824 0.004	0.914	0.569	0.087	1.899	4.400	1.082
5	Jovanovic	Q_{max} (mg g^{-1}) K_J (L mg^{-1})	8.352 -0.022	0.920	0.548	0.080	1.681	4.214	1.085

iterative method and the corresponding values of the other error functions were shown in Tables 7 to 8. In addition, Figures 8 to 13 show the fitting values of non-linear regression analysis.

Two-parameter models

Table 7 shows the values of the corresponding two-parameter isotherms obtained using the non-linear method. The result of non-linear regression method also revealed that the Temkin and Dubinin-Radushkevich isotherms fit the data in the best way respectively for NOK and MK3. It was observed that the correlation coefficient value of all isotherm models studies are very good (> 0.9), exception the Temkin model for the sample MK3, and the low χ^2, ARE, EABS and RMSE values for these adsorbents. Dubinin-Radushkevich suggests a Gaussian energy distribution onto heterogeneous surfaces (Celebi et al., 2007). Based on the energies, the variation of energy of adsorption b (kJ/mol) resulting from the non-linearization of the Temkin model is positive. A positive value of b means that the adsorption process is exothermic. Therefore, by comparison, the order of the isotherms that best fits the four sets of experimental data in this study is Dubinin-Radushkevich > Jovanovic > Langmuir > Freundlich > Temkin for MK3 and Temkin > Jovanovic Langmuir > Freundlich > Dubinin-Radushkevich.

Three-parameter models

From Table 8, Sips isotherm overlapped and seemed to be the best-fitting models for the experiment for these samples. It was observed that the correlation coefficient for all isotherms model studied are very good (> 0.9). The Sips isotherm model show high correlation coefficients value for the two adsorbents with low χ^2, ARE, EABS and RMSE values, thus indicating that the models are able to describe equilibrium data perfectly. Therefore, by comparison, the order of the isotherm best fits the four sets of experimental data in this study is Sips > Redlich-Peterson > Khan > Hill > Toth for these adsorbents. These models are suitable for predicting adsorption on heterogeneous surfaces (Ayawei et al., 2017).

Four-parameter models

Table 9 shows the values of the four corresponding isotherm parameters obtained using the non-linear method. It was observed that the correlation coefficient

Table 8. Optimum isotherm parameters and their statistical comparison values for three-parameter models.

N°	Model	Constants	Value	R^2	RMSE	χ^2	HYBRID	ARE	EABS
MK3									
1	Redlich-Peterson	A (L g^{-1})	221.901	0.956	0.363	0.027	0.686	2.509	0.878
		B (L mg^{-1})	170.344						
		β	0.573						
2	Sips	K_s (L g^{-1})	47.986	0.959	0.354	0.026	0.649	2.447	0.857
		a_s (L g^{-1})	0.026						
		β_s	2.082						
3	Toth	Q (mg g^{-1})	2.048	0.749	0.624	0.080	2.158	3.711	1.276
		K_e	0.247						
		n (mg g^{-1})	0.841						
4	Hill	Q_m (mg g^{-1})	256.773	0.975	0.362	0.027	0.680	2.500	0.875
		K_H (L g^{-1})	199.345						
		n_H	0.436						
5	Khan	Q_m (mg g^{-1})	0.405	0.956	0.363	0.027	0.683	2.505	0.877
		b_k(L g^{-1})	15.608						
		a_k	0.574						
NOK									
1	Redlich-Peterson	A (L g^{-1})	0.172	0.921	0.547	0.080	2.114	4.196	1.074
		B (L mg^{-1})	0.002						
		β	1.477						
2	Sips	K_s (Lg^{-1})	10.420	0.920	0.549	0.080	2.121	4.155	1.069
		a_s (L g^{-1})	0.013						
		β_s	0.878						
3	Toth	Q (mgg^{-1})	0.375	0.918	0.554	0.081	2.098	4.545	1.176
		K_e	0.433						
		n (mg g^{-1})	0.538						
4	Hill	Q_m (mgg^{-1})	833.736	0.915	0.555	0.081	2.111	4.560	1.172
		K_H (L g^{-1})	2403.866						
		n_H	0.725						
5	Khan	Q_m (mg g^{-1})	0.788	0.917	0.554	0.081	2.099	4.523	1.169
		b_k (L g^{-1})	0.360						
		a_k	0.299						

value of all isotherm models studied is very good (> 0.9). The result of non-linear regression method also revealed that the Baudu isotherms fit the data in the best way for NOK and MK3. This model shows the low χ^2, ARE, EABS and RMSE values for these adsorbents. On the basis of the average percentage error values (Table 9), the Baudu equation of seems better than that of Fritz–Schlunder and Marczewski–Jaroniec. The values of the maximum adsorption capacity obtained using all the three four-parameter isotherms are lower than those calculated from the Langmuir model (Tchuifon et al., 2018). Therefore, by comparison, the order of the isotherm best fits the four sets of experimental data in this study is Baudu > Jovanovic > Marczewski-Jaroniec > Fritz-Schlunder.

Conclusion

The equilibrium and kinetic study adsorption of 2,4-dinitrophenol onto activated carbon was explained using non-linear methods. Error analysis provides information

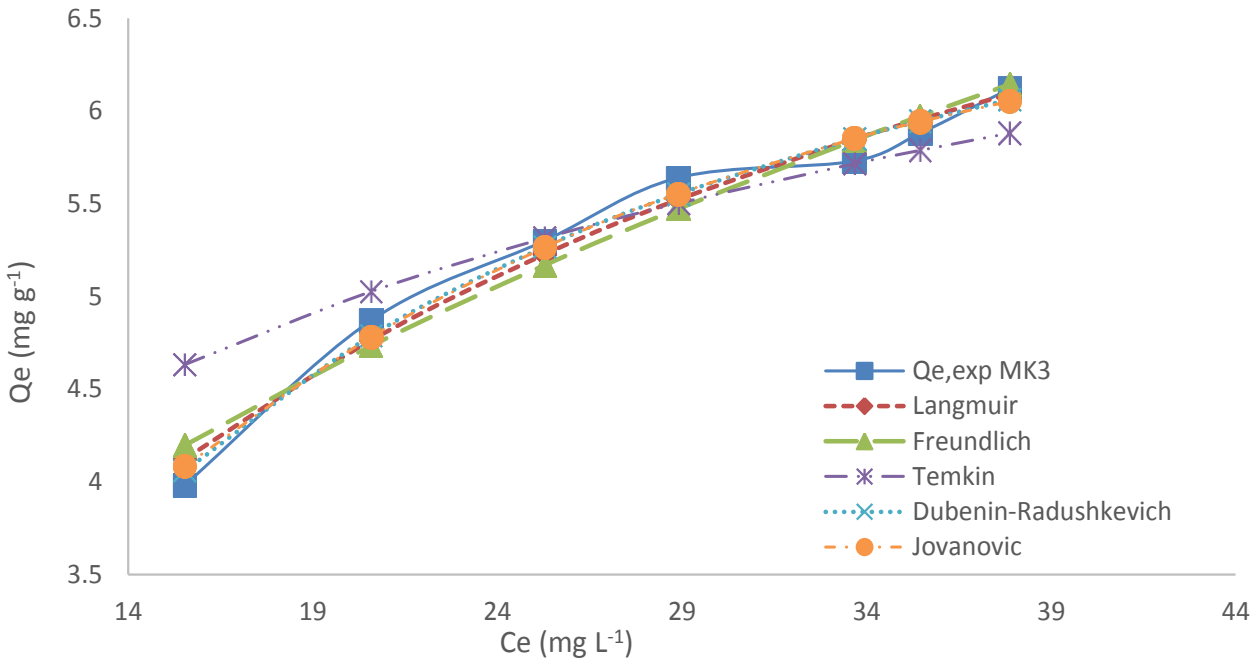

Figure 8. Comparison of measured and calculated Q_e values for two-parameter isotherms onto activated carbon MK3.

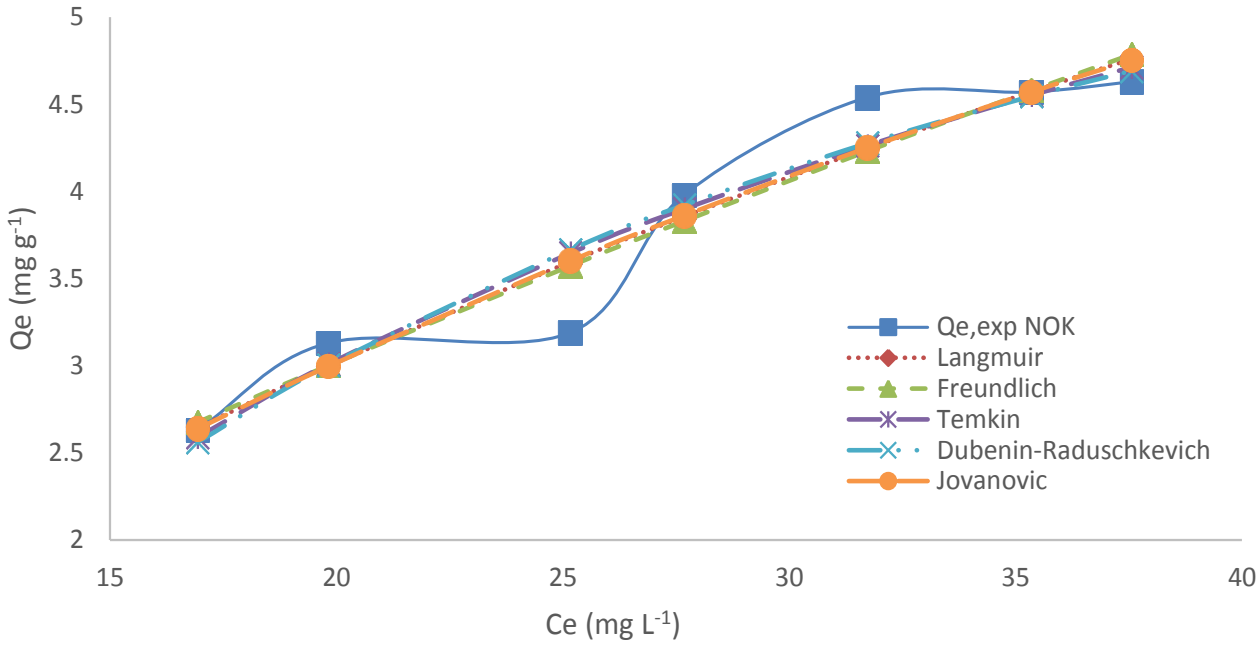

Figure 9. Comparison of measured and calculated Q_e values for two-parameter isotherms onto activated carbon NOK.

about fitness of these models on experimental data. The model with minimum error was selected best for adsorption data. In this work, the potential of two activated carbons, obtained from olive stone and mixture of cotton cakes and olive stones by chemical activation using KOH was investigated. The functional groups of these samples were determined using FTIR spectroscopy which was confirmed by using Boehm's titration and EDX analysis. XRD analysis showed that the raw material and activated carbons prepared are mainly amorphous.

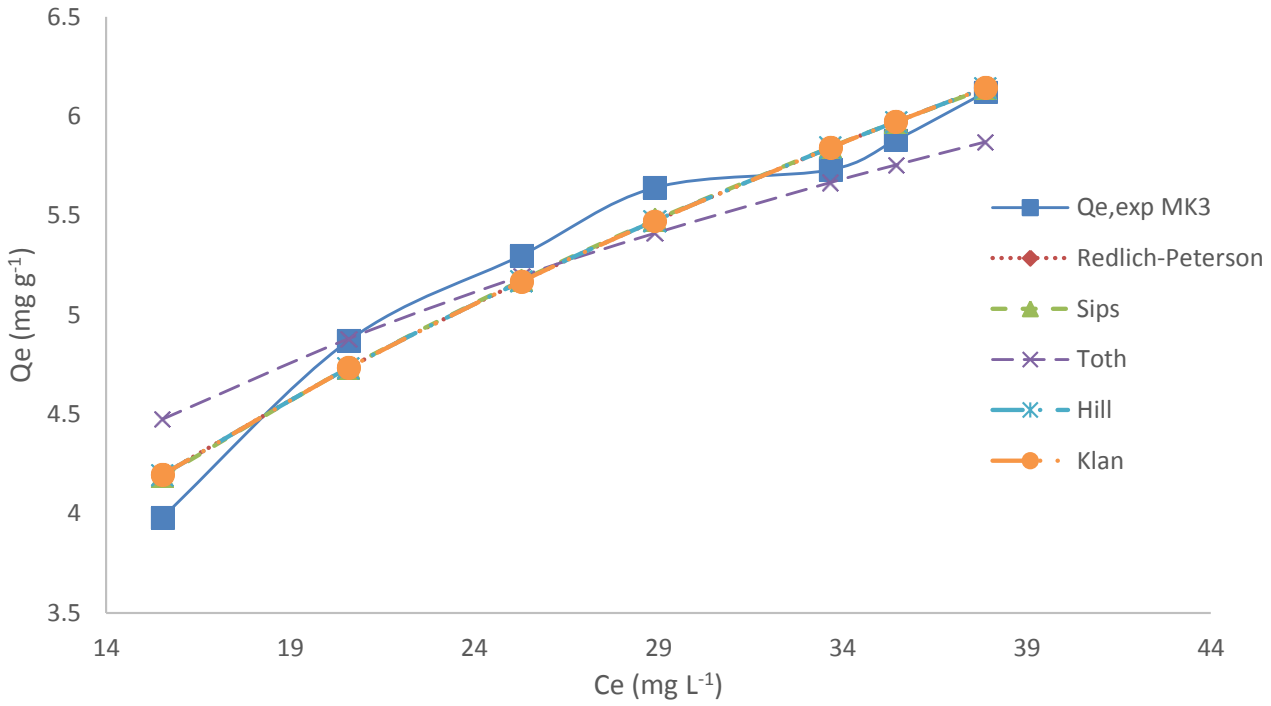

Figure 10. Comparison of measured and calculated Q_e values for three-parameter isotherms onto activated carbon MK3.

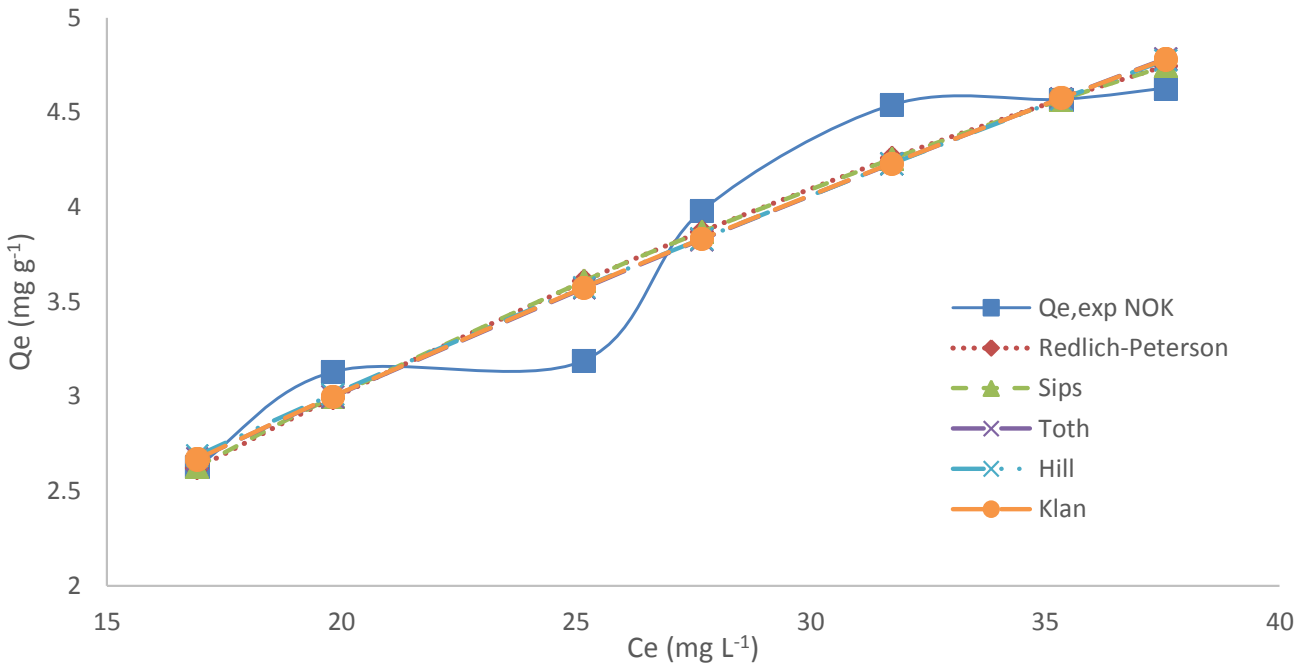

Figure 11. Comparison of measured and calculated Q_e values for three-parameter isotherms onto activated carbon CCK1.

SEM images showed an irregular and heterogeneous surface morphology with a developed and fragmented porous structure in various sizes. For all the systems examined, the Elovich kinetic model provided the best fits of the experimental data. For two parameter models Temkin and Dubinin-Radushkevich isotherms fit the

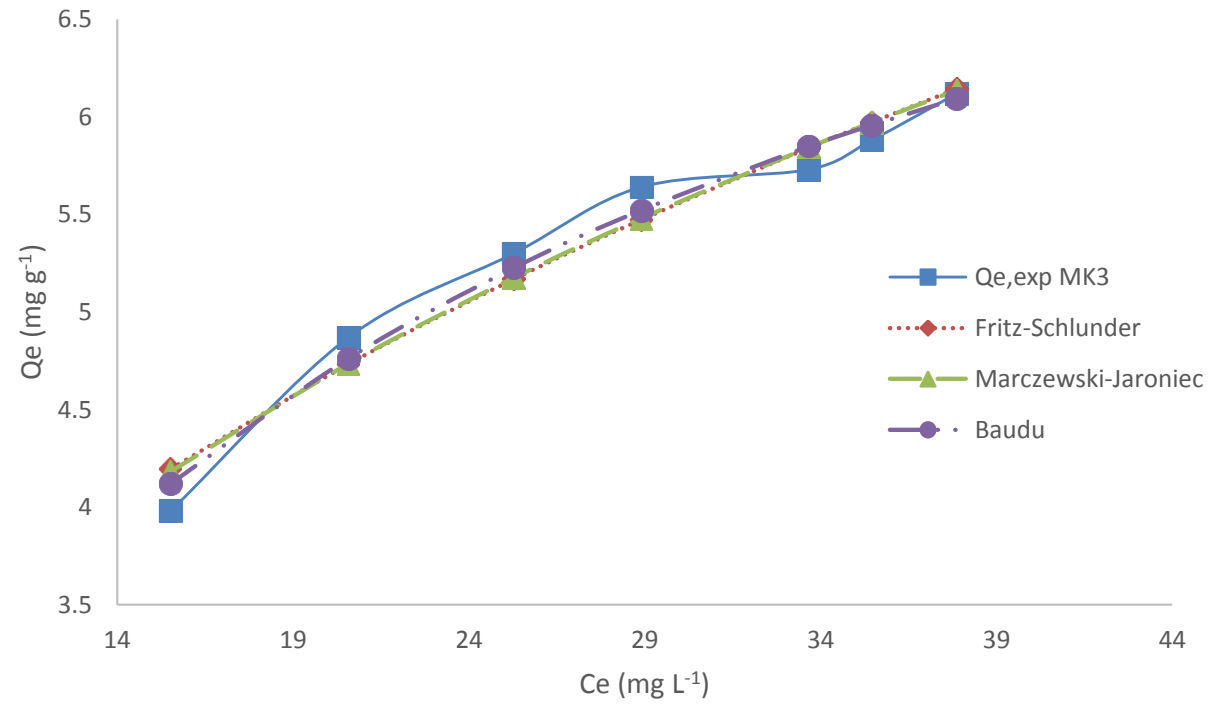

Figure 12. Comparison of measured and calculated Q_e values for four-parameter isotherms onto activated carbon MK3.

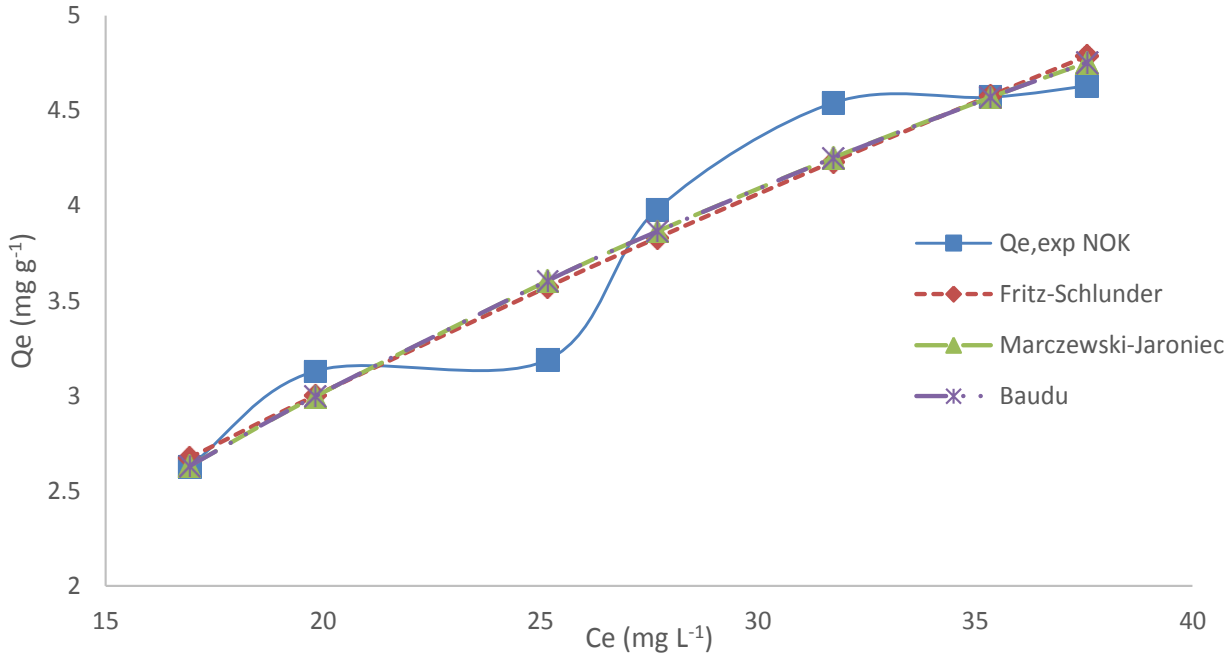

Figure 13. Comparison of measured and calculated Q_e values for four-parameter isotherms onto activated carbon NOK.

data in the best way respectively for NOK and MK3. For three-parameter models, Sips isotherm model was the best model. For four-parameters Baudu isotherms fit the data in the best way for NOK and MK3. Therefore, it can be concluded that the adsorption of 2,4-diniphenol is favorable onto NOK and MK3, and that all these activated

Table 9. Optimum isotherm parameters and their statistical comparison values for four-parameter models.

N°	Models	Constants	Values	R^2	RMSE	χ^2	hybrid	ARE	EABS
MK3									
1	Fritz-Schlunder	q_{mFS} (mg g^{-1}) K_{FS} (mg g^{-1}) q_m (mgg^{-1}) M_{FS}	40.7699 2.401 74.890 0.574	0.956	0.363	0.027	0.913	2.508	0.878
2	Marczewski-Jaroniec	q_{MMJ} (mgg^{-1}) K_{MJ} n_{MJ} M_{MJ}	221.135 0.065 0.156 0.891	0.960	0.349	0.025	0.839	2.405	0.843
3	Baudu	q_m (mg g^{-1}) b_0 x y	6.577 0.067 0.025 0.064	0.977	0.268	0.014	0.481	1.865	0.663
NOK									
1	Fritz-Schlunder	q_{mFS} (mg g^{-1}) K_{FS} (mg g^{-1}) q_m (mg g^{-1}) M_{FS}	5.79837 0.537 8.412 0.283	0.917	0.555	0.081	2.801	4.561	1.179
2	Marczewski-Jaroniec	q_{MMJ} (mg g^{-1}) K_{MJ} n_{MJ} M_{MJ}	14.250 0.030 0.786 1.345	0.919	0.549	0.080	2.828	4.179	1.078
3	Baudu	q_m (mg g^{-1}) b_0 x y	1.762 0.056 0.079 0.358	0.920	0.550	0.080	2.821	4.179	1.078

CONFLICT OF INTERESTS

The authors have not declared any conflict of interests.

REFERENCES

Abechi SE, Gimba CE, Uzairu A, Dallatu YA (2013). Preparation and Characterization of Activated Carbon from Palm Kernel Shell by Chemical Activation. Research Journal of Chemical Sciences 3:54-61.

Al-Duri B, McKay G (1988). Basic dye adsorption on carbon using a solid phase diffusion model. Chemical Engineering Journal 38:23-31.

Arvind K, Hara MJ (2015). High surface area microporous activated carbons prepared from fox nut (*Euryale ferox*) shell by zinc chloride activation. Applied Surface Science 356:753-761.

ASTM International (2006). Standard Test Method for Determination of Iodine Number of Activated Carbon: PA 19428-2959, United States 1-5.

Ayawei N, Ebelegi AN, Wankasi D (2017). Modelling and interpretation of adsorption isotherms. Journal of Chemistry ID 3039817.

Bansal RC, Donne JB, Stoeckli F (1988). Active Carbon, Marcel Dekker, Inc, New York.

Bazrafshan E, Biglari H, Mahvi A (2012). Phenol removal by electrocoagulation process from aqueous solutions. Fresenius Environment Bulletin 21:364-371.

Berardinelli S, Resini C, Arrighi L (2008). Technologies for the removal of phenol from fluid streams: a short review of recent developments. Journal of Hazardous Materials 160:265-288.

Biglari H, Afsharnia M, Alipour V, Khosravi R, Sharaf K, Mahvi A (2017). A review and investigation of the efect of nanophotocatalytic ozonation process for phenolic compound removal from real effluent of pulp and paper industry. Environmental Science and Pollution Research 24:4105-4116.

Bopda A, Tchuifon TDR, Ndifor-Angwafor GN, Kamdem TA, Anagho SG (2018). Adsorption of 2,4-dinitrophenol on activated carbon prepared from cotton cakes: Non-linear Isotherm Modeling. International Journal of Chemical Science24:1-20.

Celebi O, Uzum C, Shahwan T, Erten HN (2007). A radio-tracer study of the adsorption behavior of aqueous Ba^{2+} ions on nanoparticles of zero-valent iron. Journal of Hazardous Materials 148:761-767.

Chan L, Cheung W, Allen S, McKay G (2012). Error analysis of adsorption isotherm models for acid dyes onto bamboo derived activated carbon. Chinese Journal of Chemical Engineering 20:535-542.

Chien SH, Clayton WR (1980). Application of Elovich Equation to the Kinetics of Phosphate Release and Sorption in Soils. Soil Science

Society of America Journal 44:265-268.
Demirbas E, Kobya M, Sulak MT (2008). Adsorption kinetics of a basic dye from aqueous solutions onto apricot stone activated carbon. Bioresources Technology 99:53-68.
El-Hendawy A (2006). Variation in the FTIR spectra of a biomass under impregnation, carbonization and oxidation conditions. Journal of Analytical and Applied Pyrolysis 75:159-166.
Foo KY, Hameed BH (2010). Insights into the modeling of adsorption isotherm systems. Chemical Engineering Journal 156:2-10.
Gunay A, Arslankaya E, Tosun I (2007). Lead removal from aqueous solution by natural and pretreated clinoptilolite: adsorption equilibrium and kinetics. Journal of Hazardous Materials 146:362-371.
Hamdaoui O, Naffrechoux E, Sptil J, Fachinger C (2005). Ultrasonic desorption of *p*-chlorophenol from granular activated carbon. Chemical Engineering Journal 106:153-161.
Ho YS (2004). Citation review of Lagergren kinetic rate equation on adsorption reactions. Scientometrics 59:171-177.
Ho YS, McKay G (1998). A comparison of chemisorption kinetic models applied to pollutant removal on various sorbents. Process Safety and Environmental Protection 6:332-340.
Junxiong L, Lan W (2009). Comparison between linear and non-linear forms of pseudo first-order and pseudo-second-order adsorption kinetic models for the removal of methylene blue by activated carbon. Front. Environmental Science and Engineering in China 3:320-324.
Khalil TE, Altaher H, Reda AR (2016). Adsorptive removal of Cu (II) ions by date pits: kinetic and equilibrium studies. Environmental Engineering and Management Journal 15:2719-2732.
Kuete TIH, Tchuifon TDR, Doungmo G, Anagho SG (2018). Preparation and characterization of activated carbons from bitter kola (*Garcinia kola*) nut shells by chemical activation method using H_3PO_4; KOH and $ZnCl_2$. Chemical Sciences International Journal 23:1-15.
Lillo-Ródenas M, Cazorla-Amorós D, Linares-Solano A (2003). Understanding chemical reactions between carbons and NaOH and KOH: an insight into the chemical activation mechanism. Carbon 41:267-275.
Luan J, Plaisier A (2004). Study on treatment of wastewater containing nitrophenol compounds by liquid membrane process. Journal of Membrane Science 229:235-239.
McKay G, Mesdaghinia A, Nasseri S, Hadi M, Aminabad MS (2014). Optimum isotherms of dyes sorption by activated carbon: fractional theoretical capacity and error analysis. Chemical Engineering Journal 251:236-247.
Miranda EJ, McIntyre IM, Parker DR, Gary RD, Logan BK (2006). Two deaths attributed to the use of 2, 4-dinitrophenol. Journal of Analytical Toxicology 30:219-222.
Mubarik S, Saeed A, Mehmood Z, Iqbal M (2012). Phenol adsorption by charred sawdust of sheesham (Indian rosewood; Dalbergiasissoo) from single, binary and ternary contaminated solutions. Journal of the Taiwan Institute of Chemical Engineers 43:926-933.
Muhammad MA (2018). Equilibrium and Kinetics Study for Adsorption of 2,4-Dinitrophenol from Aqueous Solutions by Using Cucumis Sativus Peels and Kidney Bean Shells as New Low-cost Adsorbents. Applied Ecology and Environmental Sciences 6:70-78.
Ndi JS, Ketcha JM, Anagho SG, Ghogomu JN, Bilibi EPD (2014). Physical and chemical characteristics of activated carbon prepared by pyrolysis of chemically treated cola nut (*cola acuminata*) shells wastes and its ability to adsorb organics. International Journal of Advances Chemistry and Technology 3:1-13.
Ndifor-Angwafor GN, Bopda A, Tchuifon TDR, Ngakou SC, Kuete TIH, Anagho SG (2017). Removal of Paracetamol from Aqueous Solution by Adsorption onto Activated Carbon Prepared from Rice Husk. Journal of Chemical and Pharmaceutical Research 9:56-68.
Ngakou CS, Ngomo HM, Anagho SG (2018). Batch Equilibrium and Effects of Ionic Strength on Kinetic Study of Adsorption of Phenacetin from Aqueous Solution Using Activated Carbon Derived from a Mixture of *Ayous* Sawdust and *Cucurbitaceae* Peelings. Current Journal of Applied Science and Technology 26:1-24.
Okieimen FE, Okiemen CO, Wuana RA (2007). Preparation and characterization of activated carbon from rice husks. Journal of the Chemical Society 32:126-136.
Omri A, Benzina M (2012). Characterization of activated carbon prepared from a new raw lignocellulosic material: ziziphusspinachristi seeds. Journal of the Tunisian Chemical Society 14:175-183.
Pongener C, Kibami D, Rao K, Goswamee RL, Sinha D. (2015). Synthesis and characterization of activated carbon from the biowaste of the plant *Manihot esculenta.* Chemical Science Transactions 4:59-68
Rania F, Yousef NS (2015). Equilibrium and Kinetics studies of adsorption of copper (II) on natural Biosorbent. International Journal of Chemical Engineering and Applications 6:319-324.
Ringot D, Lerzy B, Chaplain K, Bonhoure JP, Auclair E, Larondelle Y (2007). In vitro biosorption of ochratoxin A on the yeast industry by-products: comparison of isotherm models. Bioresources Technology 98:1812-1821.
Sahira J, Bhadra PP (2013). Preparation and Characterization of Activated Carbon from lapsi (*Choerospondias axillaris*) Seed Stone by Chemical Activation with Potassium Hydroxide. Journal of the Institution of Engineers 9:79-88.
Sugumaran P, Priya VS, Ravichandran P, Seshadri S (2012). Production and Characterization of Activated Carbon from Banana Empty Fruit Bunch and Delonixregia Fruit Pod. Journal of Sustainable Energy and Environment 3:125-132.
Tchieda VK, Tonle IK, Tertis MC, Ngameni E, Jitaru M (2010). Adsorption of 2,4-dinitrophenol and 2,6-dinitrophenolonto organoclays and inorganic-organicpillared clays. Environmental Engineering and Management Journal 9:953-960.
Tchuifon TDR, Anagho SG, Ketcha JM, Ndifor-Angwafor GN, Ndi JN (2014). Kinetics and equilibrium studies of adsorption of phenol in aqueous solution onto activated carbon prepared from rice and coffee husks. International Journal of Engineering and Technical Research 2(10):166-173
Tchuifon TDR, Ndifor-Angwafor GN, Bopda A, Anagho SG (2018). Modeling of phenol adsorption isotherm onto activated carbon by non-linear regression methods: models with three and four parameters. Desalination and Water Treatment 136:199-206.
Virote B, Srisuda S, Wiwut T (2005). Preparation of activated carbons from coffee residue for the adsorption of formaldehyde. Separation and Purification Technology 42:159-168.
Weber WJ, Morris JC (1963). Kinetic of adsorption of carbon from solution. Journal of the Sanitary Engineering Division 89:31-63.
Yaneva ZL, Koumanova KB, Georgieva NV (2013). Linear and Nonlinear Regression Methods for Equilibrium Modelling of p-Nitrophenol Biosorption by Rhizopusoryzae: Comparison of Error Analysis Criteria. Journal of Chemistry ID 517631.
Zhao J, Yang L, Li F, Yu R, Jin C (2009). Structural evolution in the graphitization process of activated carbon by high-pressure sintering. Carbon 47:744-751.